PHYSICAL REVIEW B **66**, 035413 (2002)

Abnormal anti-Stokes Raman scattering of carbon nanotubes

Shu-Lin Zhang,[1,*] Xinhua Hu,[2] Hongdong Li,[1] Zujin Shi,[3] Kwok To Yue,[1] Jian Zi,[2] Zhennan Gu,[2] Xiaohua Wu,[1]
Zilong Lian,[1] Yong Zhan,[1] Fumin Huang,[1] Lixia Zhou,[1] Yaogang Zhang,[4] and Sumio Iijima[4]
[1]*Department of Physics, Peking University, Beijing 100871, China*
[2]*Surface Physics Laboratory, Fudan University, Shanghai 200433, China*
[3]*Department of Chemistry, Peking University, Beijing 100871, China*
[4]*Fundamental Research Laboratory, NEC Corporation, 34 Miyukigaoka Tsukuba, Baraki, 305-8501, Japan*

(Received 12 April 2002; published 22 July 2002)

Abnormal anti-Stokes Raman scattering (AASR) was unambiguously observed in carbon nanotubes (CNT's). In contrast to traditional Raman scattering theory, the absolute value of the Raman frequency of the anti-Stokes peak is not the same as that of the corresponding Stokes peak. It was demonstrated that AASR scattering originates from the unique nanoscale cylindrical structure of CNT's that can be considered naturally as a graphite structure with an intrinsic defect from its rolling. The double-resonance Raman scattering theory was applied to interpret the scattering mechanism of the AASR phenomenon successfully and quantitatively.

DOI: 10.1103/PhysRevB.66.035413 PACS number(s): 78.30.Hv, 63.22.+m, 63.50.+x

Since carbon nanotubes (CNT's) have unique electronic[1,2] and mechanical[3] properties, they can give rise to interesting consequences and potentially novel applications. CNT's are also ideal one-dimensional nanoscale structures that can be used in fundamental research for low-dimensional physics including Raman spectroscopy. Raman spectroscopy has provided very useful information in the understanding of CNT's.[4] In Raman spectroscopy, there is a well-accepted fundamental characteristic:[5] the absolute value of the Raman frequency of the anti-Stokes peak is identical to that of the corresponding Stokes peak. Tan *et al.* reported a discrepancy between the Stokes and anti-Stokes frequencies of the D^* mode in highly oriented pyrolytic graphite (HOPG) and the D mode in Si-implanted HOPG.[6] However, there is no mention that the spectrometer has been calibrated and thus their results may need additional verification as the wave number range covering Stokes and anti-Stokes positions of graphite is very wide. Recently, Kneipp *et al.* reported a discrepancy between the Stokes and anti-Stokes frequencies of the phonon mode of CNT's excited at 633 nm, but they attribute the observation to the asymmetry of the line shapes.[7] There is no unambiguous observation of a discrepancy between the Stokes and anti-Stokes frequencies of the first-order D phonon mode in undoped and unimplanted graphite material. Recently, Thomsen and Reich[8] and Sood, Gupta, and Asher[9] forwarded different models of the double-resonance Raman scattering (DRRS) theory to discuss the theoretical basis of the dependence of the D band of graphite on excitation wavelength. Both reports postulated that a natural application of the DRRS process predicts that a difference in Stokes and anti-Stokes frequencies is expected in disorder graphite, but they did not consider CNT's. In this paper we report the first unambiguous observation of an "abnormal" anti-Stokes Raman (AASR) scattering in CNT's—a discrepancy between the Stokes and anti-Stokes frequencies of the D mode. The DRRS mechanism is applied to CNT's to understand AASR scattering.

Single-wall CNT (SWCNT) samples were made by the dc-arc-discharge method using Y/Ni catalysts. The samples were purified by various methods.[10] Raman measurements were done with a Renishaw 1000 Raman microscope. Excitation wavelengths of 515, 633, and 782 nm were used. Typical resolution of the instrument is 1–2 cm^{-1} depending on the excitation wavelength used. To accurately compare the frequency of the Stokes and anti-Stokes peaks (covering over 3000–5000 cm^{-1}), a precise frequency position is crucial. Two considerations were undertaken. First, the wave number calibration of the Raman spectrometer at the region of interest was done using standard spectral lines. Second, spectrometer dispersion, i.e., the different detection efficiency of the spectrometer at different wave numbers, has been corrected. Spectral parameters were extracted by a least-squares fitting to the Lorentzian line shape(s). To describe AASR scattering, we define the frequency difference between the anti-Stokes and corresponding Stokes lines as $\Delta = |\omega_{\mathrm{AS}}| - |\omega_{\mathrm{S}}|$, where ω_{S} and ω_{AS} are the Raman frequency of the Stokes and anti-Stokes peaks, respectively. $\Delta = 0$ corresponds to normal Raman behavior.

Raman spectra in both the Stokes and anti-Stokes regions excited at 515, 633, and 782 nm are shown in Fig. 1. The shapes of the Stokes and anti-Stokes G peaks excited at 515

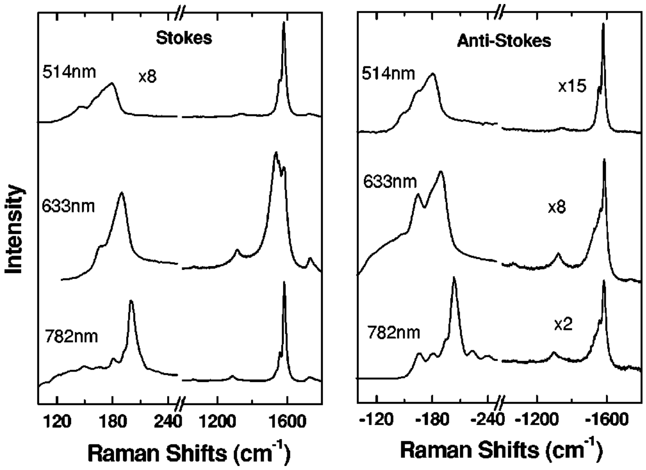

FIG. 1. Stokes and anti-Stokes Raman spectra of SWCNT's excited at 515, 633, and 782 nm.

0163-1829/2002/66(3)/035413(5)/$20.00

TABLE I. Stokes and anti-Stokes Raman frequencies and corresponding frequency difference ω_S, ω_{AS}, and Δ (cm^{-1}) of the *RB*, *D*, and *G* modes of SWCNT's and MWCNT. λ_L and *P* are the exciting wavelength in nm and the power of a 782 nm laser in %.

	λ_L/P	RB_1	RB_2	RB_3	RB_4	D	G_1	G_2	G_3
	SWCNT								
ω_S	515	179	169	160	145	1337	1582	1556	1549
	633	191	181	155		1314	1584	1556	1534
	782	202	192			1287	1585	1557	1539
	100%					1299	1578		
	50%					1299	1578		
	SWCNT								
ω_{AS}	515	−177	−169	−162	−146	−1342	−1581	−1555	−1548
	633	−191	−180	−164		−1322	−1589	−1556	−1533
	782	−203	−193			−1298	−1585	−1558	−1539
	100%					−1311	−1586		
	50%					−1312	−1590		
	SWCNT								
Δ	515	−2	0	+2	+1	+5	−1	−1	−1
	633	0	−1	−2		+8	+5	0	−1
	782	+1	−1			+11	0	+1	0
	100%					+14	+1		
	50%					+13	+1		
	MWCNT								
	633					+7	−1		

and 782 nm are characteristics of semiconducting CNT's.[11] In contrast, the spectra excited at 633 nm show asymmetric line shapes and are indicative of metallic and semiconducting CNT's in the Stokes and anti-Stokes regions, respectively.[11] Raman frequencies and corresponding Δ values extracted from Lorentzian fits for the three excitation wavelengths are listed in Table I. Typical Lorentzian fits are shown in Fig. 2. The *RB* and *G* modes consist of multiple peaks, labeled as RB_1, RB_2, RB_3, RB_4 and G_1, G_2, G_3, respectively. On the other hand, the *D* peak can be adequately fitted by only one peak, making it easier to compare individual Stokes peak with its corresponding anti-Stokes peak.

Table I shows that the frequencies of all modes shift with excitation wavelength, but all Δ of the split *G* and multiple *RB* peaks are zero to within the frequency accuracy of the Raman spectrometer. This indicates no AASR scattering for the *G* and *RB* modes. The only exception is the G_1 peak in the spectrum excited at 633 nm, which is due to the asymmetry of the line shapes, as mentioned in Ref. 7. In contrast, all Δ for the *D* peak are significantly larger than zero, including the symmetric peaks in the spectra at 515 and 782 nm

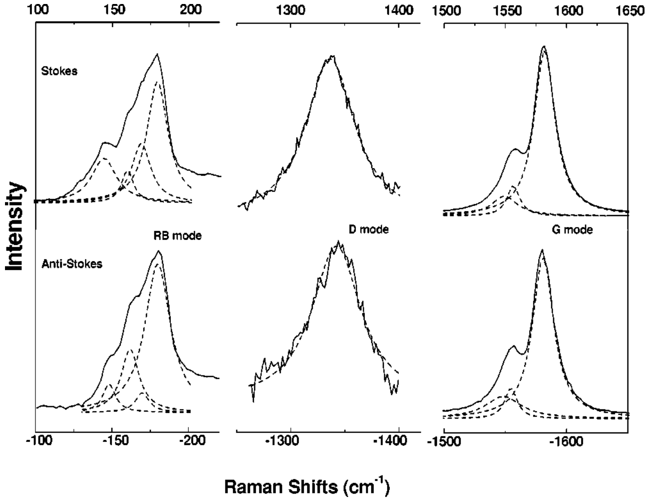

FIG. 2. Lorentzian fit of the Stokes and anti-Stokes *RB*, *D*, and *G* bands of SWCNT's excited at 515 nm.

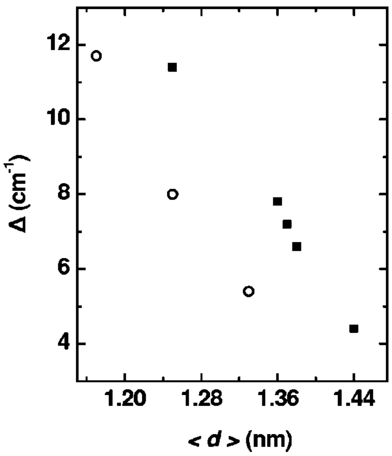

FIG. 3. Stokes and anti-Stokes Raman frequencies difference Δ vs average diameter, $\langle d \rangle$ for the *D* mode at different spots excited at 515 nm (solid square) and at the same spot excited at 616, 633, and 782 nm (open circle) for SWCNT samples.

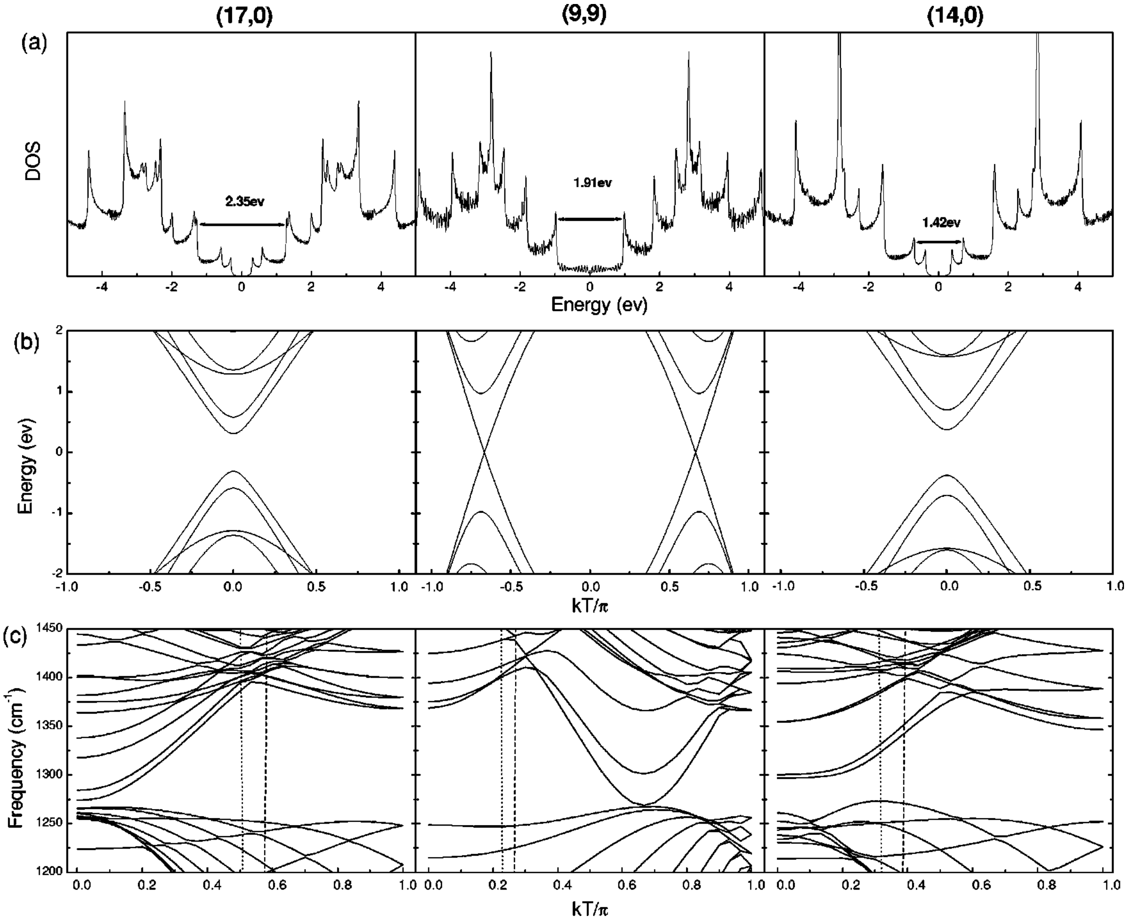

FIG. 4. Calculated electron DOS (a) and dispersion curves of the electron (b) and phonon (c) of (17,0), (9,9), and (14,0) CNT's.

excitations. Thus AASR scattering is not due to a possible artifact from the asymmetric line shape of the Stokes and/or anti-Stokes peaks.[7] Furthermore, AASR scattering exists for the *D* mode for all excitation wavelengths studied, ruling out the possibility that AASR scattering results from a strong excitation wavelength dependence of Raman peaks.[5]

The change in sample temperature induced by different laser powers can also alter Raman frequency of CNT's (Ref. 12) and may result in nonzero Δ. To understand the effect of sample temperature, the Raman spectra excited at 100% and 50% power of the 782-nm laser, i.e., at two different temperatures, were measured and the results are also listed in Table I. Indeed, the frequencies of the *D* and *G* modes are different at different excitation powers as expected,[12] but the corresponding Δ values remain the same (at $+14$, $+1$ and $+13$, -1, respectively) at the two temperatures. This indicates that AASR scattering is not affected by sample temperature.

We note that similar AASR behaviors have been observed for multiwire CNT's (MWCNT's) (Ref. 13) and the relevant result is also listed in Table I. Thus AASR scattering is present irrespective of the number of tube walls.

The above results indicate that AASR scattering in CNT's is present in the *D* mode unambiguously, independent of changes in excitation wavelength, sample temperature, or wall number of CNT's. Note that these changes do not change the global nanoscale tubular structure that is characteristic of CNT's; changing the excitation wavelength will selectively enhance tubes of different diameter,[14] while changing sample temperature can alter the C-C bond length.[12] This suggests that AASR scattering is likely to be a basic characteristic of the global nanoscale tubular structure. Furthermore, since AASR scattering is present only in Si- or Au-implanted HOPG, but not in (unimplanted) HOPG,[6,13] it is plausible to conclude that AASR scattering is related to the presence of defects. Since CNT's are essentially cylindrical tubes of nanoscale diameters formed by rolling a graphite sheet, the tubular structure can be considered a ‘‘defected’’ structure compared with the flat graphite sheet. Therefore we propose that AASR scattering in CNT's originates from the intrinsic, ‘‘defective’’ nanoscale tubular structure.

The degree of ‘‘defect’’ of nanoscale tubes can be characterized by the tube diameter *d*, i.e., the amount of deviation of the tubular structure from the flat graphite sheet. The limit $d \rightarrow \infty$ corresponds to the perfect graphite sheet, HOPG, for which there is no AASR scattering.[13] As *d* decreases, CNT's deviate more from the flat HOPG and become more defective. Thus Δ should decrease with increasing *d*, with the limit of Δ going to zero as $d \rightarrow \infty$. To probe this prediction we have measured Δ and *d* simultaneously. The result is shown in Fig. 3. Our samples do not contain CNT's with only one diameter. An average diameter $\langle d \rangle$ can be measured by the dependence of the *RB* mode on *d*.[2,15] By changing the loca-

TABLE II. Calculated and observed Stokes and anti-Stokes Raman frequencies ω_S and ω_{AS} and corresponding frequency difference Δ of (17,0), (9,9), and (14,0) CNT's.

Tube		ν (eV/q)	q	ω_S (cm^{-1})	ω_{AS} (cm^{-1})	Δ (cm^{-1})
(17,0)	Calc.	4.44	0.50	1388		
			0.58		−1349	+6
	Obs.			1337	−1342	+5
(9,9)	Calc.	7.92	0.22	1399		
			0.27		−1408	+9
	Obs.			1314	−1322	+8
(14,0)	Calc.	4.49	0.32	1324		
			0.39		−1342	+18
	Obs.			1287	−1298	+11

tion of the spot illuminated by laser or the excitation wavelength, a different assembly and, thus, different $\langle d \rangle$ of CNT's are probed. Figure 3 shows the result of five different spots on the same sample excited at 515 nm, and at the same spot on the sample, but excited at 616, 633, and 782 nm, also shown in Fig. 3. Indeed, Δ decreases with increasing $\langle d \rangle$, confirming that AASR scattering originates from the global nanoscale tubular structure of CNT's.

To understand the scattering mechanism of the AASR phenomenon, the diameter, symmetry, and electron and phonon structures of CNT samples are examined. From the integrated intensity ratio in Fig. 1, we found that the most prominent *RB* mode in the multiple *RB* modes is at 179, 190, and 202 cm^{-1} in the spectra excited at 488, 633, and 782 nm, respectively. The structure of the dominant CNT can be found from the peak position.[2,15] Thus, using the nomenclature of Ref. 2 (*n*,*m*) of the predominant tubes are (17,0), (9,9), and (14,0) in the spectra excited at 488, 633, and 782 nm, respectively, with corresponding diameters of 13.0, 12.4, and 11.5 nm, respectively. The density of state (DOS) of electron and dispersion curves of electron and phonon for (17,0), (9,9), and (14,0) tubes were calculated[16–18] and are shown in Fig. 4. In these calculations, the nearest-neighbor C-C overlap energy γ_0 is taken to be 2.78 eV and lattice dynamic parameters are taken to be $\varphi_r^{(1)}=36.50$, $\varphi_r^{(2)}=8.80$, $\varphi_r^{(3)}=3.00$, $\varphi_r^{(4)}=1.92$, $\varphi_{ti}^{(1)}=24.50$, $\varphi_{ti}^{(2)}=-3.23$, $\varphi_{ti}^{(3)}=-5.25$, $\varphi_{ti}^{(4)}=2.29$, $\varphi_{to}^{(1)}=9.82$, $\varphi_{to}^{(2)}=-0.40$, $\varphi_{to}^{(3)}=0.15$, and $\varphi_{to}^{(4)}(4)=-0.58$. Based on the calculated results, the following characteristics can be deduced for these CNT's. First, the electron DOS of the (17,0), (9,9), and (14,0) tubes exhibit an electron transition at energies 2.35, 1.91, and 1.42 eV, respectively. This is consistent with our measurements indicating that the Raman spectra excited at 515 nm (2.54 eV), 633 nm (1.96 eV), and 782 nm (1.59 eV) are due to in-resonant Raman scattering (RRS). Second, although only the electron dispersion of the (9,9) tube exhibits metallic characteristic, the semiconducting electron dispersions of (17,0) and (14,0) tubes also show linear band characteristics with Fermi velocities $\nu_1=\nu_2=\nu$ in the RRS energy region. Third, the phonon dispersions of the *D* mode for these tubes do not increase linearly with the wave vector q in the entire Brillouin zone, but increase monotonically with q in a narrow region of the zone. These characteristics are similar to those of electron and phonon dispersions that can result in the DRRS proposed by Thomsen and Reich,[8] suggesting that DRRS may be applicable in the RRS process here. Furthermore, the intrinsic tubular-defect structure of CNT's acts as the necessary lattice defect needed for electrons to scatter elastically in the DRRS process, further implying that DRRS and then AASR scattering is possible in CNT's.

To further investigate whether the DRRS theory can give quantitative results for AASR scattering in CNT's, frequencies of the *D* modes were estimated from the theory. The theoretical values were obtained by utilizing the quasimomentum selection rule[8]

$$q=(E_1-\hbar\omega_{ph})/-\nu_1 \quad \text{or} \quad (E_1-\hbar\omega_{ph})/\nu_2, \tag{1}$$

together with the phonon dispersion relationship

$$\omega_{ph}(q)=f(q), \tag{2}$$

where E_1, ω_{ph}, $\hbar$, ν_1, and ν_2 are the incident photon energy, phonon frequency, Planck's constant, and Fermi velocity, respectively. Anti-Stokes scattering corresponds to replacing ω_{ph} in Eq. (1) by $-\omega_{ph}$. The graphic method was used and the lowest-energy dispersion curve was utilized to solve Eqs. (1) and (2). The calculated and observed ω_S and ω_{AS} and corresponding Δ of (14,0), (9,9), and (17,0) CNT's are listed in Table II. The errors between calculated and experimental values are within 3%–6% for ω_S and ω_{AS}, while they coincide qualitatively for Δ. Therefore, the agreement between calculated and experimental results is quite good, indicating that the proposed DRRS mechanism can be used to interpret the AASR phenomenon.

In conclusion, we report on an unambiguous observation of a discrepancy between the absolute frequency of the anti-Stokes peak and that of the corresponding Stokes peak for the *D* mode of carbon nanotubes (AASR scattering). We propose that AASR scattering is related to the global nanoscale tubular structure which can be treated as an intrinsic defect. Based on calculations of electron DOS and dispersion relation of the electron and phonon, AASR scattering is adequately explained by an expansion of the DRRS theory. AASR scattering of CNT's is a phenomenon of intrinsic significance originating from the nanoscale tubular structure of CNT's with their unique electron and phonon properties.

We gratefully thank Professor P. Yu for repeated, detailed, and helpful discussions. The authors would also like to thank Professor M. S. Dresselhaus and Professor M. Cardona for constructive discussions. We acknowledge the support from NSFC (of China) under Program Nos. 69476037, 19774009, and 69876001 and The State Commission of Science and Technology of China.

*To whom correspondence should be addressed. Electronic address: slzhang@pku.edu.cn

[1] S. Iijima, Nature (London) **354**, 56 (1991).

[2] R. Saito, G. Dresserlhaus, and M. S. Dresserlhaus, *Physical Properties of Carbon Nanotubes* (Imperial College Press, London, 1998).

[3] M. Nardelli, B. Yakobson, and J. Bernholc, Phys. Rev. Lett. **81**, 4656 (1998).

[4] M. S. Dresselhaus *et al.*, in *Proceedings of the 17th International Conference on Raman Spectroscopy, Beijing, China, 2000,* edited by Shu-Lin Zhang and Banfen Zhu (Wiley, New York, 2000), p. 9.

[5] D. A. Long, *Raman Spectroscopy* (McGraw-Hill, New York, 1977).

[6] P. H. Tan, Y. M. Deng, and Q. Zhao, Phys. Rev. B **58**, 5435 (1998).

[7] K. Kneipp, H. Kneipp, P. Corio, S. D. M. Brown, K. Shafer, J. Motz, L. T. Perelman, E. B. Hanlon, A. Marucci, G. Dresselhaus, and M. S. Dresselhaus, Phys. Rev. Lett. **84**, 3470 (2000).

[8] C. Thomsen and S. Reich, Phys. Rev. Lett. **85**, 5214 (2000).

[9] A. K. Sood, R. Gupta, and S. A. Asher, J. Appl. Phys. **90**, 4494 (2001).

[10] Z. Shi, Y. Lian, X. Zhou, Z.Gu, Y. Zhang, S. Iijima, L. Zhou, K. T. Yue, and S.-l. Zhgang, Carbon **37**, 1449 (1999).

[11] M. A. Pimenta, A. Marucci, S. A. Empedocles, M. G. Bawendi, E. B. Hanlon, A. M. Rao, P. C. Eklund, P. C. Eklund, R. E. Smalley, G. Dresselhaus, and M. S. Dresselhaus, Phys. Rev. B **58**, R16 016 (1998).

[12] H. D. Li, K. T. Yue, Z. L. Y. Zhan, S.-L. Zhang, Z. Shi, Z. Gu, Y. Zhang, and S. Iijima, Appl. Phys. Lett. **76**, 2053 (2000).

[13] F. Huang, K. T. Yue, T. Pingheng, S.-L. Zhang, Z. Shsi, X. Zhou, and Z. Gu, Chin. J. Light. Scattering, **10**, 10 (1998); S.-L.Zhang, F. Huang, L. Zhou, Y. Zhan, K. T. Yue, Z. Shi, X. Zhou, and Z. Gu, *ibid.* **11**, 110 (1999).

[14] A. M. Rao, E. Richter, S. Bandow, B. Chase, P. C. Elkund, K. A. Woillams, S. Fang, K. R. Subbaswamy, M. Mennon, A. Thess, R. E. Samlley, K. R. Subbaswamy, M. Menon, A. Thess, R. E. Smalley, G. Dresselhaus, and M. Dresselhaus, Science **275**, 187 (1997).

[15] A. Jorio, R. Saito, J. H. Hafner, C. M. Lieber, M. Hunter, T. McClure, G. Dresselhaus, and M. S. Dresselhaus, Phys. Rev. Lett. **86**, 1118 (2001).

[16] R. A. Jishi, L. Venkataraman, M. S. Dresselhaus, and G. Dresselhaus, Chem. Phys. Lett. **209**, 77 (1993).

[17] R. A. Jishi, D. Inomata, K. Nakao, M. S. Dresslhaus, and G. Dresselhaus, J. Phys. Soc. Jpn. **63**, 2252 (1994).

[18] R. Saito, G. Dresselhaus, and M. S. Dresslhaus, Phys. Rev. B **61**, 2981 (2000).